

Exclusive top production at a Linear Collider at and off the threshold

JÜRGEN REUTER^{1a}, FABIAN BACH^{2b}, BIJAN CHOKOUFÉ NEJAD^{3a}, ANDRE HOANG^{4c,d},
WOLFGANG KILIAN^{5e}, JONAS LINDERT^{6f}, STEFANO POZZORINI^{7g}, MAXIMILIAN
STAHLHOFEN⁸, THOMAS TEUBNER⁹ⁱ, CHRISTIAN WEISS^{10a}

^a*DESY Theory Group, Notkestr. 85, D-22607 Hamburg, Germany*

^b*European Commission, Eurostat, 2920 Luxembourg*

^c*University of Vienna, Faculty of Physics, Boltzmannngasse 5, A-1090 Wien, Austria*

^d*Erwin Schrödinger International Institute for Mathematical Physics, University of Vienna,
Boltzmannngasse 9, A-1090 Vienna, Austria*

^e*University of Siegen, Department of Physics, Walter-Flex-Str. 3, D-57068 Siegen, Germany*

^f*Institute for Particle Physics Phenomenology, Ogden Centre for Fundamental Physics,
Department of Physics, University of Durham, Durham DH1 3LE, United Kingdom*

^g*Physik-Institut, Universität Zürich, Winterthurerstrasse 190, CH-8057 Zürich, Switzerland*

^h*PRISMA Cluster of Excellence, Institute of Physics, Johannes Gutenberg University,
Staudingerweg 7, D-55128 Mainz, Germany*

ⁱ*University of Liverpool, Department of Mathematical Sciences, Liverpool L69 3BX, United
Kingdom*

*Talk presented by Jürgen Reuter at the International Workshop on Future
Linear Colliders (LCWS2017), Strasbourg, France, 23-27 October 2017.
C17-10-23.2.*

ABSTRACT

We review exclusive top pair production including decays at a future high-energy lepton collider, both in the threshold region and for higher energies. For the continuum process, we take complete QCD next-to-leading order matrix elements for the $2 \rightarrow 6$ process with leptonic W decays into account. At threshold, we match the fixed-order relativistic QCD-NLO cross section to a nonrelativistic cross section with next-to-leading logarithmic (NLL) threshold resummation implemented via a form factor.

1 Introduction

Top physics is one of the standard pillars of the physics program of any future high-energy lepton collider. The rationale is to determine the properties of the heaviest Standard Model (SM) quark, its mass, its width and its couplings to a level of accuracy that is not possible at hadron colliders like Tevatron and the LHC, and to use the top quark as a handle to search for physics beyond the Standard Model. Here, we review recent work on the precision calculation of the QCD next-to-leading order (QCD-NLO) for off-shell top quark production, including (leptonic) W -decays, in the continuum [1]. The details of this calculation and the results will be discussed in Sec. 2. As shown in this section, the perturbative fixed-order calculation yields naive K factors of three and more in the kinematic region close to the top-antitop production threshold for top-pair production, or better $WbWb$ or $\ell\nu\ell\nu b\bar{b}$ production. In the threshold region, fixed-order perturbation theory in the strong coupling α_s is not a good approximation anymore, but the top velocity v is an additional expansion parameter and Coulomb-singular terms $\sim (\alpha_s/v)^n$ and (ideally also) large logarithms $\sim (\alpha_s \log v)^n$ have to be resummed. In recent work [2], we used a previously known effective field theory setup based on non-relativistic QCD (NRQCD) to compute a form factor accounting for the resummation of the threshold-singular terms at NLL accuracy, implemented it in the fixed-order calculation and matched the result to the QCD-NLO cross section in the transition region between threshold and continuum. We thus obtained a fully-differential cross section, which gives reliable predictions for all center-of-mass energies. Depending on how inclusive the process is, we achieve LL + QCD-NLO (for very exclusive processes) or NLL + QCD-NLO precision (for inclusive processes) in the threshold region. This will be discussed in Sec. 3. Finally, we summarize and give an outlook in Sec. 4.

2 Continuum calculation

We first discuss the relativistic QCD-NLO corrections to the off-shell top pair production in the continuum, i.e. away from the production threshold. This means, investigating either the process $e^+e^- \rightarrow W^+bW^- \bar{b}$ or $e^+e^- \rightarrow \ell^+e^- \bar{\nu}_e \mu^+ \nu_\mu b\bar{b}$ including leptonic W decays. Looking at the full four- or six-particle final state, there are double-resonant diagrams included (involving a top and an anti-top propagator), single-resonant diagrams and non-resonant irreducible background processes.

In order to study the QCD-NLO corrections for the top production processes discussed here, we take the WHIZARD framework for (QCD-)NLO processes. WHIZARD [3] is a multi-purpose event generator. It comes with its own matrix-element generator for tree-level amplitudes,

¹juergen.reuter@desy.de

²fabian.bach@desy.de

³bijan.chokoufe@desy.de

⁴andre.hoang@univie.ac.at

⁵kilian@physik.uni-siegen.de

⁶jonas.m.lindert@durham.ac.uk

⁷pozzorin@physik.uzh.ch

⁸mastahlh@uni-mainz.de^h

⁹thomas.teubner@liverpool.ac.uk

¹⁰christian.weiss@desy.de

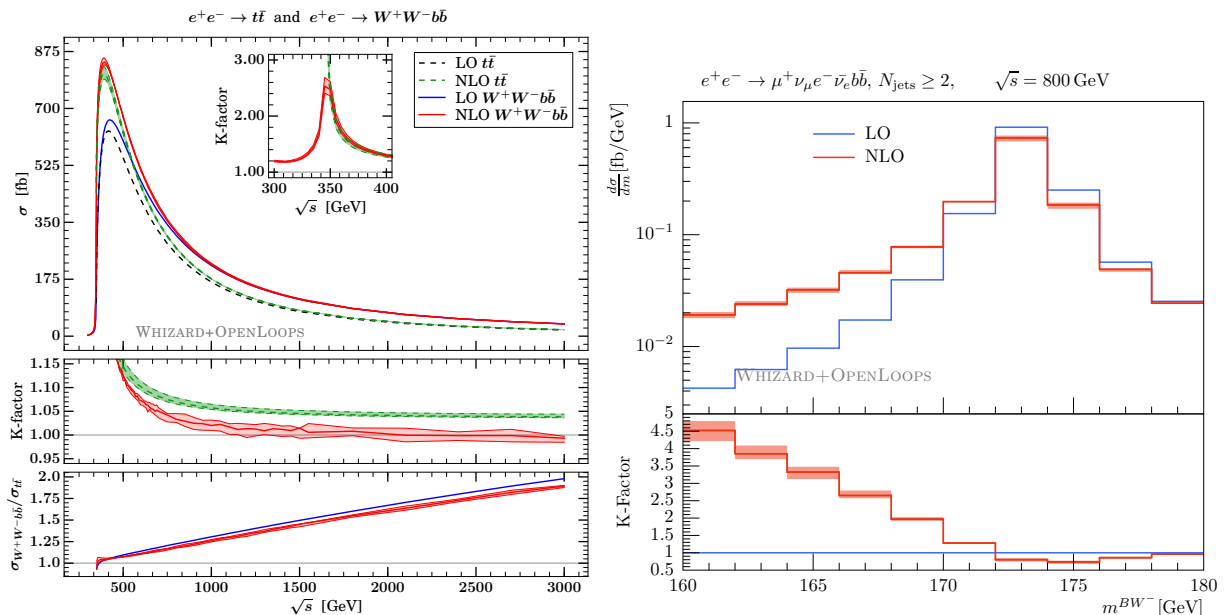


Figure 1: Total cross section for the process $e^+e^- \rightarrow W^+W^-b\bar{b}$ as a function of the center-of-mass energy (left); the upper ratio plot in the bottom shows the K factor, the lower one the ratio of the four-body process to on-shell $t\bar{t}$ production. The inset shows the K factor enhancement in the threshold region. Fully off-shell leptonic $t\bar{t}$ production ($e^+e^- \rightarrow e^-\bar{\nu}_e\mu^+\nu_\mu b\bar{b}$) differential distribution (right). Blue is LO, red is QCD-NLO including scale variations. Schemes and input parameters as described in the text.

0'Mega [4,5] which supports almost arbitrary models like e.g. supersymmetry [6] and many more. External models can be used inside WHIZARD by its interface to FeynRules [7]. For the QCD color decomposition, WHIZARD uses the color-flow formalism [8], and it comes with its own parton shower implementation [9]. The work on QCD-NLO within WHIZARD started with a hard-coded implementation for the production of b jets at LHC [10,11], while matching between resummed terms and fixed-order calculations have been tackled by combining fixed-order electroweak corrections to chargino production at the ILC with an all-order QED initial-state structure function [12,13]. Since quite recently, WHIZARD is able to do automatic POWHEG matching for e^+e^- processes [14].

For (QCD-)NLO processes, WHIZARD automatically sets up FKS subtraction [15] and generates the corresponding phase space for all the singular emission regions. Here we take virtual matrix elements, which contain up to pentagon integrals for the processes considered here, as well as the color-correlated and spin-correlated matrix elements for the collinear and soft splittings, respectively, from the OpenLoops one-loop provider (OLP) [16,17,18]. For the amplitudes, we take the complex mass scheme using complexified masses $\mu_i^2 = m_i^2 + im_i\Gamma_i$, which leads e.g. to a complex weak mixing angle. The input values are as follows: $m_W = 80.385$ GeV, $m_Z = 91.1876$ GeV, $m_t = 173.2$ GeV, $m_H = 125$ GeV, and we perform the calculation here and for the threshold with massive b -quarks of $m_b = 4.2$ GeV. It is important that the widths used in the calculation are at the same order and in the same scheme than the scattering process in order to guarantee properly normalized branching ratios: $\Gamma_Z^{\text{LO}} = 2.4409$

GeV, $\Gamma_Z^{\text{NLO}} = 2.5060$ GeV, $\Gamma_W^{\text{LO}} = 2.0454$ GeV, $\Gamma_W^{\text{NLO}} = 2.0978$ GeV, $\Gamma_{t \rightarrow Wb}^{\text{LO}} = 1.4986$ GeV, $\Gamma_{t \rightarrow Wb}^{\text{LO}} = 1.3681$ GeV, $\Gamma_{t \rightarrow f\bar{f}b}^{\text{LO}} = 1.4757$ GeV, $\Gamma_{t \rightarrow f\bar{f}b}^{\text{NLO}} = 1.3475$ GeV. Note that for the process with stable W s, $e^+e^- \rightarrow W^+W^-b\bar{b}$, one has to take the total top width for two-body decays, while for the full process, $e^+e^- \rightarrow e^-\bar{\nu}_\ell\mu^+\nu_\mu b\bar{b}$ the total top width for three-body decays. For the Higgs boson we take the value $\Gamma_H = 4.31$ MeV. As the matrix elements for the full off-shell processes contain narrow resonances, particularly the $H \rightarrow b\bar{b}$ resonance, we use a resonance-aware version of the FKS subtraction formalism to make sure that cancellations between real emissions and subtraction terms do cancel though the real emission could shift the kinematics on or off the resonance compared to Born kinematics. This resonance-aware treatment is automatically done in **WHIZARD**. As we are using massive b -quarks, no cuts are necessary for the process $e^+e^- \rightarrow W^+W^-b\bar{b}$, but the process $e^+e^- \rightarrow e^-\bar{\nu}_\ell\mu^+\nu_\mu b\bar{b}$ exhibits a collinear singularity from photon emission off the electron line going from the initial to the final state. The integrations for the full QCD-NLO are very stable. We did two independent own integrations with the serial and the non-blocking MPI-parallelizable version of VAMP [19] inside **WHIZARD**, and we confirmed the result within **Sherpa** [20] and **Munich**.

For the QCD-NLO corrections, we take the top mass as renormalization scale. The scale variations for the process $e^+e^- \rightarrow W^+bW^-b$ is very small, at the level of two per cent. After one has replaced the top width in the matrix elements by a running top width $\Gamma_t(\mu_R)$, the scale variations for the on-shell process $e^+e^- \rightarrow t\bar{t}$ behave the same way as for the off-shell process. In Fig. 1 we show in the left panel the total cross section for $e^+e^- \rightarrow W^+bW^-b$ as a function of the center-of-mass energy \sqrt{s} over the whole kinematic range from well below the threshold up to full energy stage of CLIC at 3 TeV. Below the main plot there are two ratio plots, the first showing the K factor $\sigma(\text{NLO})/\sigma(\text{LO})$, the second showing the ratio of the off-shell to the on-shell process, $\sigma(e^+e^- \rightarrow W^+bW^-b)/\sigma(e^+e^- \rightarrow t\bar{t})$. In the upper ratio plot, the green curve is the K factor for the on-shell process, while the red one is the K factor for the off-shell process. For the off-shell process, the K factor tends to almost unity at a TeV and beyond. The second ratio plot shows that without restricting to single- and double resonant phase-space regions, the background processes start to more and more dominate over the signal top-pair production. The colors in the second ratio plot correspond to the legend, i.e. blue for LO and red for NLO. The inset in the left plot of Fig. 1 shows the enhancement in the K factor around the top threshold where fixed-order perturbation theory is not a valid approximation any more, cf. Sec. 3. The K factor for the on-shell process even becomes infinite here. In the right panel of Fig. 1 we show as an example for a differential distribution the invariant mass for the negatively charged W (reconstructed at Monte Carlo truth level) and the b jet for the full process $e^+e^- \rightarrow e^-\bar{\nu}_\ell\mu^+\nu_\mu b\bar{b}$ at the center-of-mass energy of $\sqrt{s} = 800$ GeV where the cross section peaks. The LO distribution is shown in blue and the QCD-NLO distribution including scale variations in red. One clearly sees that the K factor is not constant over the phase space. Particularly for low invariant masses below the top mass peak, there is a large enhancement as this part of the phase space gets populated massively by gluon radiation off the top peak region.

Note that the setup inside **WHIZARD** allows to immediately do QCD-NLO calculations and simulations for polarized cross sections, or include QED initial-state photon radiation as well as effects from beamspectra. In Ref. [1], we also calculated the processes $e^+e^- \rightarrow t\bar{t}H$, $e^+e^- \rightarrow W^+bW^-bH$ and $e^+e^- \rightarrow e^-\bar{\nu}_\ell\mu^+\nu_\mu b\bar{b}H$ at QCD-LO and QCD-NLO, which we omitted in this proceedings article here.

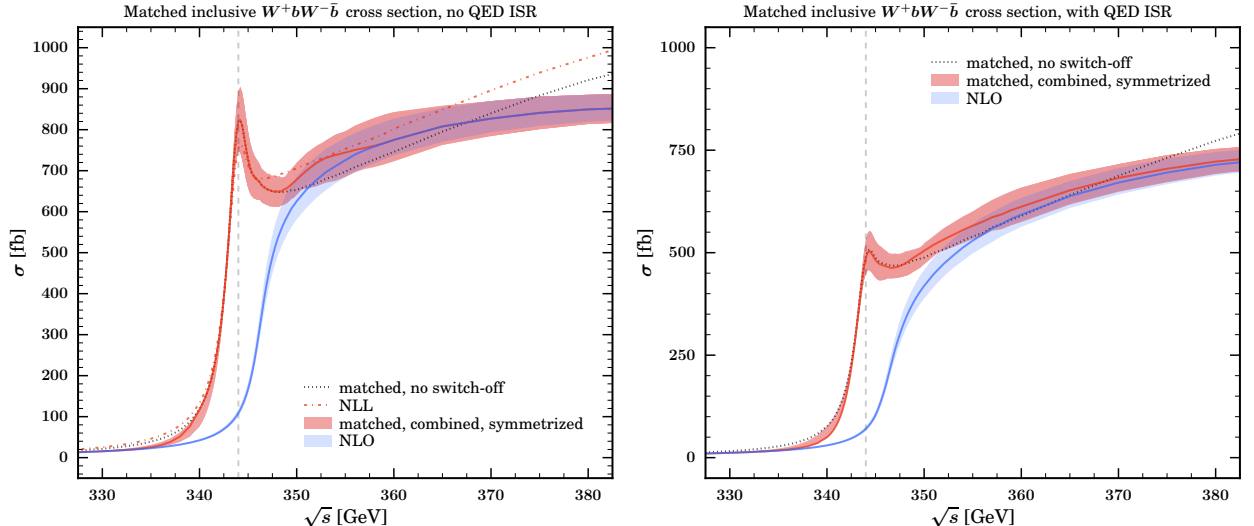


Figure 2: Matched NRQCD-NLL + QCD-NLO calculation without (left) and with (right) QED ISR. The dashed vertical line is the value of twice M^{1S} . Blue is the fixed QCD-NLO calculation, red is the fully matched calculation. The matched calculation has a full envelope over (symmetrized) scale uncertainties as well as variations over switch-off functions.

3 Threshold matching

A kinematic fit to the shape of the rising of the cross section at the top threshold is believed to be the most precise method to measure the top quark mass with an ultimate precision of 30-80 MeV. For this the systematic uncertainties of the experimental measurement – especially the details of the beam spectrum – as well as the theoretical uncertainties have to be well under control. As shown Sec. 2, close to the kinematical threshold for the on-shell production of a $t\bar{t}$ pair, fixed-order perturbation theory is not a good approximation. Very close to threshold, the effective field theory of (v/p)NRQCD separates the hard scale m_t , the soft scale given by the top momentum of the non-relativistic top quark with velocity v , $m_t v$ and the ultrasoft scale, given by the kinetic energy of the top quark, $m_t v^2$ and allows to resum large logarithms of v with $\alpha_s \sim v \sim 0.1$ close to threshold. ”Fixed-order” calculations resumming only Coulomb singularities, but no velocity logarithms, for the totally inclusive $t\bar{t}$ production have been carried out in NRQCD to NNNLO [21]. The large velocity logarithms have been resummed to next-to-next-leading logarithmic (NNLL) [24] order (cf. also [22,23] for predictions which did not contain the full set of NNLL ultrasoft logarithms). These NRQCD calculations are based on the optical theorem and hold only for the total inclusive cross section and in a narrow window around the $t\bar{t}$ threshold. We report here about work where we combined and matched the NLL NRQCD-resummed process close to the top threshold with the fixed-order (relativistic) QCD-NLO process in the continuum. By a carefully performed matching procedure, our approach smoothly interpolates between the threshold region and the continuum, and it allows to study all kinds of differential distributions.

The matching is embedded into the `WHIZARD-OpenLoops` QCD-NLO fixed-order framework discussed in Sec. 2. The NLL resummed NRQCD contributions are included in terms of (S-/P-wave) form factors to the (vector/axial vector) $\gamma/Z - t - \bar{t}$ vertex. These form factors are

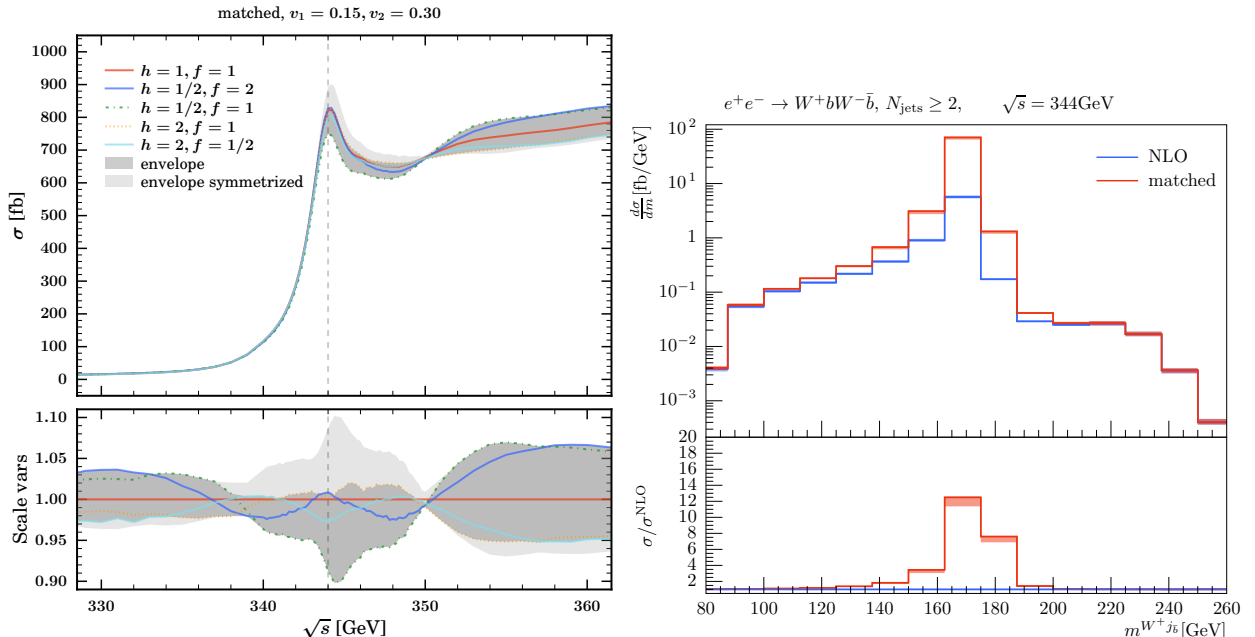


Figure 3: *Left panel: Matched NRQCD-NLL + QCD-NLO total cross section as on the left of Fig. 2, but for a single choice of switch off-function. h and f are renormalization scale parameters as defined in [2,24]. The grey bands display the corresponding scale variations with and without symmetrization. Right panel: Wb invariant mass distribution at threshold ($\sqrt{s} = 344$ GeV) as obtained with **WHIZARD**. The red line represents the full NRQCD-NLL + QCD-NLO matched, and the blue line the pure QCD-NLO result. The associated bands are generated by the same scale variations as in the left panel, here without symmetrization.*

obtained from the numerical solution of Schrödinger-type equations for the NLL Green functions computed by the **Toppik** [25,26,27] code, which is included in **WHIZARD**. The technical details of their implementation and the matching setup can be found in [2]. In order to avoid double-counting between the fixed-order QCD-NLO part and the resummed NLL-NRQCD part, one has to expand the form factors to first order in α_s and subtract those pieces. As the NRQCD resummed calculations are not available for the 5-point functions $\gamma^*/Z^* \rightarrow W^+bW^-\bar{b}$, but only for the top-vector and axial-vector currents, this removal of double-counting has to be done in a factorized approach within a double-pole approximation. There is no trivial gauge-invariant subset for the process $e^+e^- \rightarrow W^+bW^-\bar{b}$. In order to maintain gauge-invariance of the factorized amplitudes, an on-shell projection of the exclusive final states to the top mass shell is performed. The technical details, especially concerning the direction of the three-momenta and the definition of the on-shell projection below the kinematical threshold can be found in [2]. The implementation inside **WHIZARD** has been validated with analytical calculations for different invariant mass cuts on the reconstructed top quarks from Ref. [28].

As for larger values of the top velocity ($v \gtrsim 0.4$) only the relativistic QCD-NLO result is valid, we define a switch-off function that smoothly interpolates between the two regions. This function is in principle arbitrary, and the possibility to vary this function and its parameters adds another theory uncertainty on top of the different scale variations in the different kinematic regimes. For technical details again, we refer to [2]. The results of our matching procedure

are displayed in Fig. 2. These plots show the total inclusive cross section for the process $e^+e^- \rightarrow W^+bW^-\bar{b}$, in the left panel without and in the right panel with QED initial-state radiation (ISR). The dashed vertical line gives the value for $2M^{1S}$. The 1S mass M^{1S} is defined as half of the perturbative mass of a would-be 1S toponium state and represents a renormalon free short-distance mass, which we treat as an input parameter in WHIZARD. The blue line shows the QCD-NLO cross section including scale variations in the blue shaded areas. The only difference to the results in Sec. 2 is a different renormalization, see [2]. The red curve shows the NRQCD-NLL + QCD-NLO result, while the shaded band contains all (symmetrized) scale variations of the hard, soft and ultrasoft factorization/renormalization scales according to [24] as well as variations of the switch-off function to a reasonable extent [2]. The dotted black line shows the matched results without applying a switch-off function to the factorized NRQCD terms which deviates above threshold from the relativistic QCD-NLO result. In Fig. 3, left panel, we see the matched result in the threshold region for a single choice of switch-off parameters, but scale variations over the full two-dimensional renormalization parameter range defined in [24]. This shows that the scale variation bands for the resummed NLL result in the threshold region are highly asymmetric with respect to the central value which motivates to apply a symmetrization of the error bands around the central value. This symmetrization is also shown in Fig. 2. In the right panel of Fig. 3 we show as an example for a differential distribution the invariant mass of the $W - b$ jet system. Blue is the fixed-order QCD-NLO distribution, while red is the fully matched distribution including scale variations, here un-symmetrized. The ratio plot in the bottom does not show a K factor, but the ratio of the matched result to the QCD-NLO fixed order result. It shows an enhancement in the top mass peak due to threshold resummation by a factor of ten to twelve.

4 Summary and Outlook

We presented work on the QCD-NLO corrections for exclusive top-quark pair production including top and (leptonic) W decays. Kinematic regions in the continuum up to the highest available energies of CLIC were covered as well as the threshold region. Both calculations have been performed in the QCD-NLO framework of the WHIZARD event generator which allows to include all important physics of a lepton collider like polarization, QED ISR radiation and non-trivial beam spectra. The continuum calculations represent the first massive $2 \rightarrow 6$ and $2 \rightarrow 7$ QCD-NLO calculations for lepton colliders. The matched threshold calculation smoothly interpolates the threshold region described by non-relativistic QCD to the relativistic QCD-NLO calculation and constitutes the highest available precision available at the level of the completely exclusive final state. While the work presented here is more a proof-of-principle of the matching procedure between threshold and continuum, it is obvious that the various differential distributions (which are accessible now and of which we only showed one here) offer plenty of possibilities for top mass measurements. This is part of ongoing and future work. Other directions for future work are the matching at even higher order in QCD, the inclusion of electroweak corrections to the relativistic continuum process, and the inclusion of W decays also in the matched calculations.

Acknowledgments

JRR wants to thank the organizers of LCWS 2017 in Strasbourg for a great conference at a lovely venue. JRR, BCN and CW acknowledge support from the Collaborative Research Unit (SFB) 676 of the DFG, projects B1 and B11. We like to thank Stefan Kallweit for his help with the cross-checks by the `Munich` code.

References

- [1] B. Chokouf Nejad, W. Kilian, J. M. Lindert, S. Pozzorini, J. Reuter and C. Weiss, *JHEP* **1612**, 075 (2016) doi:10.1007/JHEP12(2016)075 [[arXiv:1609.03390](#) [hep-ph]].
- [2] F. Bach, B. C. Nejad, A. Hoang, W. Kilian, J. Reuter, M. Stahlhofen, T. Teubner and C. Weiss, [arXiv:1712.02220](#) [hep-ph].
- [3] W. Kilian, T. Ohl and J. Reuter, *Eur. Phys. J. C* **71**, 1742 (2011) doi:10.1140/epjc/s10052-011-1742-y [[arXiv:0708.4233](#) [hep-ph]].
- [4] M. Moretti, T. Ohl and J. Reuter, [hep-ph/0102195](#).
- [5] B. Chokoufe Nejad, T. Ohl and J. Reuter, *Comput. Phys. Commun.* **196**, 58 (2015) doi:10.1016/j.cpc.2015.05.015 [[arXiv:1411.3834](#) [physics.comp-ph]].
- [6] T. Ohl and J. Reuter, *Eur. Phys. J. C* **30**, 525 (2003) doi:10.1140/epjc/s2003-01301-7 [[hep-th/0212224](#)].
- [7] N. D. Christensen, C. Duhr, B. Fuks, J. Reuter and C. Speckner, *Eur. Phys. J. C* **72**, 1990 (2012) doi:10.1140/epjc/s10052-012-1990-5 [[arXiv:1010.3251](#) [hep-ph]].
- [8] W. Kilian, T. Ohl, J. Reuter and C. Speckner, *JHEP* **1210**, 022 (2012) doi:10.1007/JHEP10(2012)022 [[arXiv:1206.3700](#) [hep-ph]].
- [9] W. Kilian, J. Reuter, S. Schmidt and D. Wiesler, *JHEP* **1204**, 013 (2012) doi:10.1007/JHEP04(2012)013 [[arXiv:1112.1039](#) [hep-ph]].
- [10] T. Binoth, N. Greiner, A. Guffanti, J. Reuter, J.-P. Guillet and T. Reiter, *Phys. Lett. B* **685**, 293 (2010) doi:10.1016/j.physletb.2010.02.010 [[arXiv:0910.4379](#) [hep-ph]].
- [11] N. Greiner, A. Guffanti, T. Reiter and J. Reuter, *Phys. Rev. Lett.* **107**, 102002 (2011) doi:10.1103/PhysRevLett.107.102002 [[arXiv:1105.3624](#) [hep-ph]].
- [12] W. Kilian, J. Reuter and T. Robens, *Eur. Phys. J. C* **48**, 389 (2006) doi:10.1140/epjc/s10052-006-0048-y [[hep-ph/0607127](#)].
- [13] T. Robens, J. Kalinowski, K. Rolbiecki, W. Kilian and J. Reuter, *Acta Phys. Polon. B* **39**, 1705 (2008) [[arXiv:0803.4161](#) [hep-ph]].

- [14] J. Reuter, B. Chokoufe, A. Hoang, W. Kilian, M. Stahlhofen, T. Teubner and C. Weiss, *J. Phys. Conf. Ser.* **762**, no. 1, 012059 (2016) doi:10.1088/1742-6596/762/1/012059 [[arXiv:1602.06270](#) [hep-ph]].
- [15] S. Frixione, Z. Kunszt and A. Signer, *Nucl. Phys. B* **467**, 399 (1996) doi:10.1016/0550-3213(96)00110-1 [[hep-ph/9512328](#)].
- [16] F. Cascioli, P. Maierhofer and S. Pozzorini, *Phys. Rev. Lett.* **108**, 111601 (2012) doi:10.1103/PhysRevLett.108.111601 [[arXiv:1111.5206](#) [hep-ph]].
- [17] F. Buccioni, S. Pozzorini and M. Zoller, [[arXiv:1710.11452](#) [hep-ph]].
- [18] F. Buccioni, S. Pozzorini and M. Zoller, [[arXiv:1801.03772](#) [hep-ph]].
- [19] T. Ohl, *Comput. Phys. Commun.* **120**, 13 (1999) doi:10.1016/S0010-4655(99)00209-X [[hep-ph/9806432](#)].
- [20] T. Gleisberg, S. Hoeche, F. Krauss, M. Schonherr, S. Schumann, F. Siegert and J. Winter, *JHEP* **0902**, 007 (2009) doi:10.1088/1126-6708/2009/02/007 [[arXiv:0811.4622](#) [hep-ph]].
- [21] M. Beneke, Y. Kiyo, P. Marquard, A. Penin, J. Piclum and M. Steinhauser, *Phys. Rev. Lett.* **115**, no. 19, 192001 (2015) doi:10.1103/PhysRevLett.115.192001 [[arXiv:1506.06864](#) [hep-ph]].
- [22] A. H. Hoang, A. V. Manohar, I. W. Stewart and T. Teubner, *Phys. Rev. D* **65**, 014014 (2002) doi:10.1103/PhysRevD.65.014014 [[hep-ph/0107144](#)].
- [23] A. Pineda and A. Signer, *Nucl. Phys. B* **762**, 67 (2007) doi:10.1016/j.nuclphysb.2006.09.025 [[hep-ph/0607239](#)].
- [24] A. H. Hoang and M. Stahlhofen, *JHEP* **1405**, 121 (2014) doi:10.1007/JHEP05(2014)121 [[arXiv:1309.6323](#) [hep-ph]].
- [25] M. Jezabek, J. H. Kuhn and T. Teubner, *Z. Phys. C* **56**, 653 (1992). doi:10.1007/BF01474740
- [26] R. Harlander, M. Jezabek, J. H. Kuhn and T. Teubner, *Phys. Lett. B* **346**, 137 (1995) doi:10.1016/0370-2693(94)01668-3 [[hep-ph/9411395](#)].
- [27] A. H. Hoang and T. Teubner, *Phys. Rev. D* **60**, 114027 (1999) doi:10.1103/PhysRevD.60.114027 [[hep-ph/9904468](#)].
- [28] A. H. Hoang, C. J. Reisser and P. Ruiz-Femenia, *Phys. Rev. D* **82**, 014005 (2010) doi:10.1103/PhysRevD.82.014005 [[arXiv:1002.3223](#) [hep-ph]].